RESEARCH ARTICLE

WILEY ENERGY RESEARCH

Performance enhancement of dye-sensitized solar cells via cosensitization of ruthenizer Z907 and organic sensitizer SQ2

M. Younas[1,2] (iD) | M.A. Gondal[1,2] (iD) | U. Mehmood[4] | K. Harrabi[1,3] | Z.H. Yamani[1,2] |
F.A. Al-Sulaiman[3]

[1] Laser Research Group, Department of Physics, King Fahd University of Petroleum and Minerals (KFUPM), P.O. Box 5047, Dhahran 31261, Saudi Arabia

[2] Center of Research Excellence in Nanotechnology (CENT), KFUPM, Dhahran, Saudi Arabia

[3] Center of Research Excellence in Renewable Energy (CoRERE), KFUPM, Dhahran, Saudi Arabia

[4] Polymer Engineering Department, University of Engineering and Technology (UET), Lahore, Pakistan

Correspondence
M. A. Gondal, Laser Research Group, Department of Physics, King Fahd University of Petroleum and Minerals (KFUPM), P. O. Box 5047, Dhahran 31261, Saudi Arabia.
Email: magondal@kfupm.edu.sa

Summary

Cosensitization is a highly effective technique to enhance the photovoltaic performance of a dye-sensitized solar cell. The main objective of this work is to improve the performance of dye-sensitized solar cell using cosensitization approach and investigation of the effect of the organic cosensitizer concentration on the power conversion efficiency of the fabricated solar cell devices. In this work, Z907, a ruthenium dye, has been cosensitized with SQ2, an organic sensitizer, and an overall efficiency of 7.83% has been achieved. The fabricated solar cells were evaluated using UV-Vis spectroscopy, current-voltage (I-V) characteristics, and electrochemical impedance spectroscopy analysis. Our results clearly indicate that the concentration of organic cosensitizer strongly affects the photovoltaic performance of fabricated solar cells. Upon optimization, the cell fabricated with 0.3 mM Z907 + 0.2 mM SQ2 dye solution demonstrated J_{sc} (mA/cm^2) = 21.38, V_{oc} (mV) = 698.37, FF (%) = 52.46, and power conversion efficiency of η (%) = 7.83 under standard AM1.5G 1 sun illumination (100 mW/cm^2). It was observed that the efficiency of cosensitized solar cells is significantly superior than that of individual sensitized solar cells (Z907 [η = 5.08%] and SQ2 [η = 1.39%]). This enhancement in efficiency could be attributed to the lower electron-hole recombination rate, decrease in competitive absorption of I^-/I^-_3, and less dye aggregation because of the synergistic effect in cosensitized solar cells.

KEYWORDS
cosensitization, DSSC, efficiency, electrochemical, photovoltaic, renewable energy

NOMENCLATURE: DSSC, Dye-sensitized solar cell; UV-Vis, Ultraviolet visible spectroscopy; IV, Current voltage; EIS, Electrochemical impedance spectroscopy; CE, Counter electrode; I^-/I^{3-}, Iodine/triiodide; mM, Millimole; FTO, Fluorine-doped tin oxide (SnO$_2$:F); TiO$_2$, Titanium dioxide; CB, Conduction band; HOMO, Highest occupied molecular orbital; LUMO, Lowest unoccupied molecular orbital; PCE, Power conversion efficiency; J_{sc}, Current density (mA/cm^2); V_{oc}, Open circuit voltage (mV); FF, Fill factor (%); η, Efficiency (%)

1 | INTRODUCTION

Energy plays an important role in modernization, automation, and economic growth of any country and society at large. Escalating energy demand and ecological issues have encouraged researchers to focus on clean and eco-friendly new energy sources.[1-3] Solar energy enjoys

the fact that it is easily attainable, most wide and approachable source of renewable energy on our planet. The annual estimated sun energy accessible on our planet is about 3×10^{24} J, which is about 10^4 times greater than that currently consumed by the world population.[4,5] Solar energy is considered among the top available alternatives to mitigate the carbon dioxide (CO_2) emission to the environment because of the burning of fossil fuels.[6-8] High emission of CO_2 into the atmosphere has caused many catastrophic effects in global warming, forest declining, and climate change. To use this energy, various kinds of photovoltaic cells have been developed since 1954. Dye-sensitized solar cells (DSSCs) are third-generation solar cells which is a quite new version of photovoltaic devices.[9] Dye-sensitized solar cell was first developed by Grätzel and coworkers in 1991. Dye-sensitized solar cells gained considerable attention because of their low cost, easy fabrication, less toxicity, and moderate power conversion efficiency (PCE) as compared to silicon-based solar cells.[10,11]

Dye-sensitized solar cells consist of 3 major components: (1) photoanode, (2) counter electrode, and (3) electrolyte. Photoanode, one of the major components of DSSC, performs two important functions: (i) collection of electrons from the photo-excited dye and their transportation to the outer circuit and (ii) acts as scaffolding which is needed for dye adsorption. Usually, anodes are porous in morphology for sufficient dye adsorption and wide band gap materials, eg, TiO_2, ZnO, Nb_2O_5, etc.[12] The main functions of the counter electrode (CE) are (i) the reduction of oxidized electrolyte because of the regeneration of dye and (ii) transportation of the positive charges (holes) toward the CE. Various types of CE have been used for DSSC including platinum (Pt), carbon nanotubes, and other carbonaceous materials.[13] Electrolyte, which is sandwiched between photoanode and CE, is one of the most important components in the DSSC. The prime function of the electrolyte is to regenerate photo-exited dye.[5] There are different types of electrolytes, eg, liquid, gel polymer, and other polymer electrolytes, which have been used in DSSC. Liquid electrolyte, eg, iodine/triiodide (I^-/I_3^-), are commonly used because of their outstanding characteristics like the couple has a good solubility, not absorbing much of the incident light, containing an appropriate redox potential and fast dye regeneration. However, because of the liquid nature, the stability, long-term durability, and performance of the DSSC are compromised. To resolve these issues, researchers replaced the liquid electrolyte with hole transport materials, gel polymer, and other polymers for stable and flexible DSSCs. Bella et al report new gel-polymer membranes doped with iodine salts for the enhancement of photovoltaic performance. Gerosa et al used Ti

grid for the fabrication of completely flexible DSSC. An important work to enhance the thermal and long-term stability of DSSC has been carried out by Bella et al by introducing the finely dispersed nanosized silica particles with the iodide/triiodide electrolytes and obtained promisingly encouraging results. The group also carried out the polymeric approach to patterning the DSSC anode, in addition with polymer electrolytes, for stable and efficient DSSC.[14-17] Photosensitizer (dye) is the main component of DSSC which is adsorbed on the semiconducting material, for instance, TiO_2 and ZnO.[18-20] The PCE of DSSC mainly depends on photosensitizer. The main function of dye in DSSC is to absorb incident photons and produce the electron-hole pairs which can be transferred to the external circuit through the semiconducting material. In the last 15 years, remarkable progress has been observed at many aspects of this technology, approaching record efficiencies over 14%.[21] However, still, there is room for efficiency enhancement of these photovoltaic devices and their commercial applications at large scale. The specific reason for low PCE is the low absorption range of photosensitizer (dye).[1,22] Presently, there is no such single sensitizer having the ability to absorb sunlight in a broad spectral range (400-900 nm).[23]

Cosensitization is a highly successful technique to boost the PCE of DSSC.[24,25] It improves the absorption spectral range, hence light harvesting efficiency of solar cells.[26] Many combinations of photosensitizers like porphyrin cosensitized with ruthenium complexes,[27] organic dye cosensitized with ruthenium complexes,[28-30] or cosensitization of phthalocyanine with an organic sensitizer,[31-33] and an organic sensitizer that has been cosensitized with different organic dyes[34,35] has been used. Kuang et al used two organic dyes (SQ1 and JK2), and found PCE of 6.4% using solvent-free electrolyte.[35] Chen et al used different organic dyes for cosensitization, a hemicyanine dye, a merocyanine dye, and a dye based on squarylium cyanine, and obtained the efficiency of 6.5%.[34] Wu et al synthesized two indolium-based organic dyes and used them in DSSCs. They used their mixture to the ratio of 1:3 and got overall PCE of 3.0% under standard 1 sun AM 1.5G illumination.[36] Lee et al used cosensitization technique for plastic DSSCs. They got PCE of 5.1% by cosensitization of ruthenium complexes (N719 and N749) and organic dye consisting of the thienylfluorene segment called FL.[37] Lan et al used zinc porphyrin dye (LD12) for cosensitization with an organic sensitizer (CD5) in a stepwise approach and obtained an efficiency of 9%.[26] Wei et al cosensitized ruthenium dye (N719) with different 3 organic dyes (DM, DE, and DP) and got an efficiency of 7%.[29]

In this work, we used the cosensitization technique to improve the efficiency of DSSC. The organic SQ2 dye was

used as a cosensitizer with ruthenium Z907 dye. Dye solutions of different concentrations were prepared and used for the sensitization of semiconductor anode. The performance of DSSCs sensitized with individual dyes (Z907 or SQ2) is compared to that of solar cell devices fabricated with cosensitized (Z907 + SQ2) phenomenon under the same conditions of fabrication. The results reveal that the overall photovoltaic performance of the optimized cosensitized solar cells is significantly enhanced, and hence, PCE is much superior than that of individually sensitized solar cells.
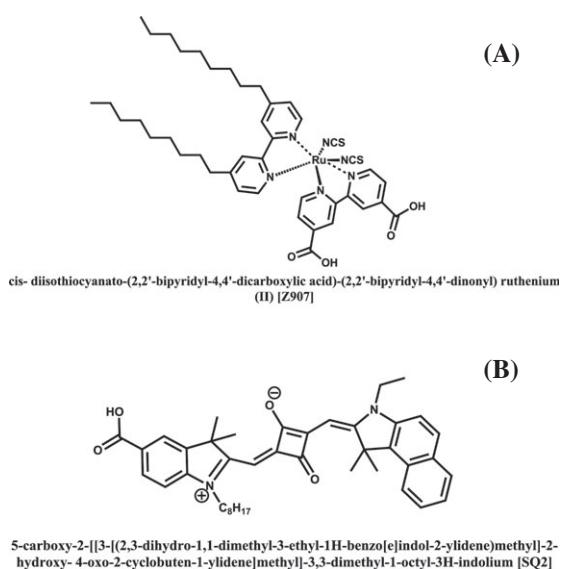
2 | FABRICATION AND CHARACTERIZATION

2.1 | Materials

Fluorine-doped tin oxide (SnO_2:F, FTO) conductive glass substrates, anatase TiO_2 paste (Solaronix, T/SP 14451), dyes (Ruthenizer 520-DN and Sensitizer SQ2), electrolyte (Solaronix, Iodolyte Z-50), and platinum paste (Solaronix, Plastisol T) were all procured from Solaronix (Switzerland).

2.2 | Preparation of dye solutions

Seven different dye solutions were prepared in ethanol, ie, 0.5 mM Z907, 0.5 mM SQ2, 0.4 mM Z907 + 0.1 mM SQ2, 0.3 mM Z907 + 0.2 mM SQ2, 0.25 mM Z907 + 0.25 mM SQ2, 0.2 mM Z907 + 0.3 mM SQ2, and 0.1 mM Z907 + 0.4 mM SQ2. The structures and chemical names of both dyes are shown in Figure 1.

(A)

cis- diisothiocyanato-(2,2'-bipyridyl-4,4'-dicarboxylic acid)-(2,2'-bipyridyl-4,4'-dinonyl) ruthenium (II) [Z907]

(B)

5-carboxy-2-[[3-[(2,3-dihydro-1,1-dimethyl-3-ethyl-1H-benzo[e]indol-2-ylidene)methyl]-2-hydroxy- 4-oxo-2-cyclobuten-1-ylidene]methyl]-3,3-dimethyl-1-octyl-3H-indolium [SQ2]

FIGURE 1 Structures and chemical names of (A) Z907 and (B) SQ2 dyes

2.3 | Fabrication of DSSC

The DSSC flow diagram is shown in Figure 5B for easy visualization. Fluorine-doped tin oxide conductive glass substrates were used with TiO_2 paste by tape casting method and then subsequently annealed at 200°C for the first 10 minutes and 450°C for the next 20 minutes. The deposited TiO_2 film thickness on each substrate was analyzed and measured with the help of SEM cross-sectional images as shown in Figure 2. Each film shows an average thickness of 9 μm. After cooling to room temperature, TiO_2-deposited FTO conductive substrates were soaked in the respective dye solutions, ie, individual and mixture of dye solution for 24 hours to obtain best photoanodes. After the sensitization, photoanodes were rinsed with methanol to remove the unadsorbed dye. Similarly, the tape casting method has been used for the preparation of platinum CEs which were prepared by tape casting of platinum paste on conductive FTO glass substrates. The samples were then annealed at 450°C for 15 minutes. The both electrodes were joined together with super glue gel (named as the original super glue by super glue corporation). Finally, the electrolyte was injected between the two joint electrodes to complete the fabrication of solar cells. In this work, the fabricated solar cells active area is 0.2 cm^2.

2.4 | Characterization of DSSCs

The spectrophotometer (model: UV/Vis JASCO-670) has been used to acquire the ultraviolet-visible (UV-Vis) spectra of prepared dye solutions and dyes anchored to TiO_2 films on FTO conductive glass. The solar simulator (IV-5, Sr #83, PV Measurement, Incorporation) at Air Mass (AM) 1.5G (1000 Wm^{-2}) with Source Meter (Keithley 2400) has been used to evaluate the IV characteristics of the fabricated DSSCs. The potentiostat VMP3 SAS (s/n: 0373 Bio-Logic Instruments) has been used to investigate the electrochemical impendence spectroscopy (EIS) properties under dark conditions of illumination, with a 10 mV amplitude AC signal having a frequency within the range of 10 Hz and 800 kHz. The applied bias was in the range of 0 and 750 mV larger than the V_{oc} of the DSSC.

3 | RESULTS AND DISCUSSION

### 3.1 | Ultraviolet (UV-Vis) spectroscopy of fabricated DSSC

The absorption spectra (UV-Vis spectra) of dyes (Z907, SQ2, and Z907 + SQ2) in ethanol and adsorbed on the surface of TiO_2 films coated on FTO conductive glass are shown in Figure 3. Three broader and intense peaks
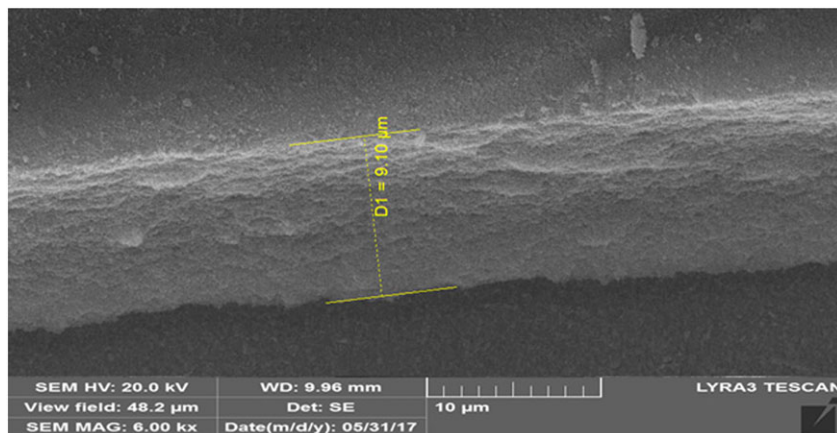
FIGURE 2 Cross-sectional image of TiO_2 film deposited on FTO glass substrate [Colour figure can be viewed at wileyonlinelibrary.com]

in Z907 at 530, 385, and 310 nm are attributed to metal to ligand charge transfer and intraligand (π-π^*) charge-transfer transitions, respectively, as shown in Figure 3A. Similarly, Figure 3B depicts the absorption spectrum of SQ2 with two absorption peak in the regions 580 to 620 and 620 to 680 nm. The peak in the region 580 to 618 nm can be ascribed to π-π^* electronic transitions of the conjugated molecules, while the second peak is because of the donor to acceptor anchoring groups' intermolecular charge transfer. Figure 3C shows the absorption spectra of mixed dyes in ethanol, which are more intense as compared to that of individual dyes. The results clearly demonstrate that the concentration of

cosensitizer strongly affects the absorption of light. The absorption of Z907 enhanced with the increase in the concentration contents of SQ2 sensitizer because of the synergistic effect of both sensitizers. However, the absorption of Z907 + SQ2 becomes red shifted when anchored to TiO_2 as shown in Figure 3D, owing to strong interaction among the carboxylate groups and the surface Ti^{4+} ions,[4] which enhances the delocalization of the π^* orbital. The red shift physically can be noted from Figure 3C, D as the peaks are shifted from 656 to 671 nm. This red shift is because of the strong interaction between carboxylate groups from dyes and Ti^{4+} ions from semiconductor TiO_2 film. Furthermore, the absorption spectrum of
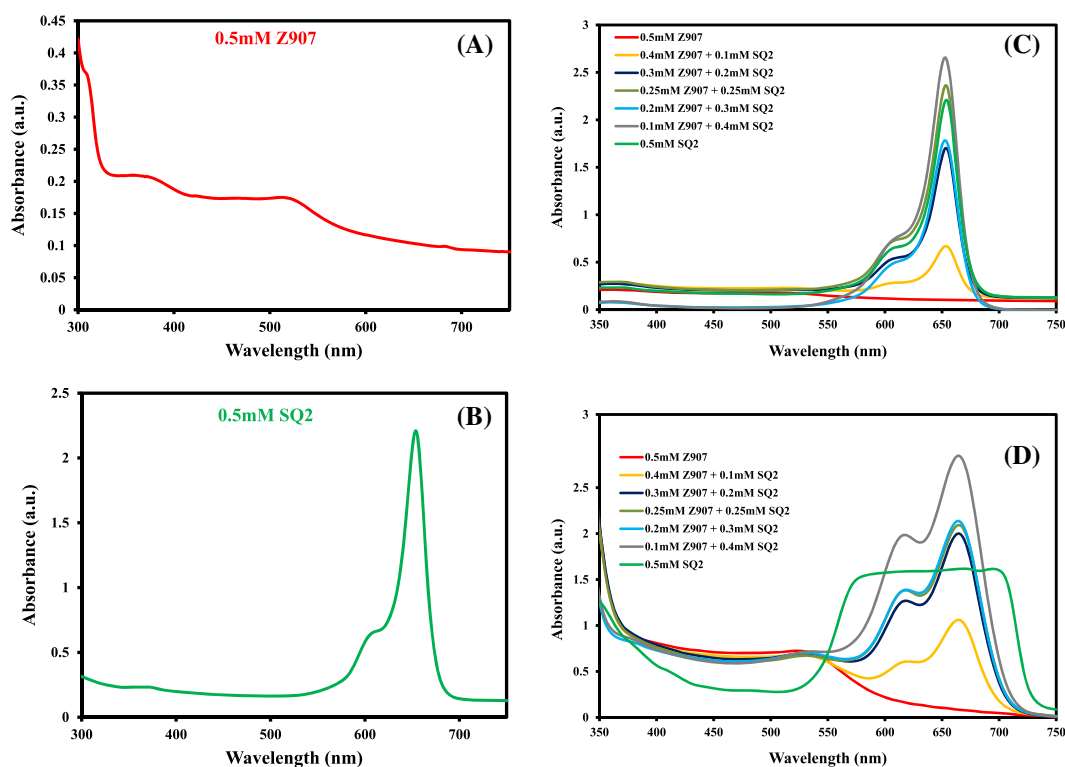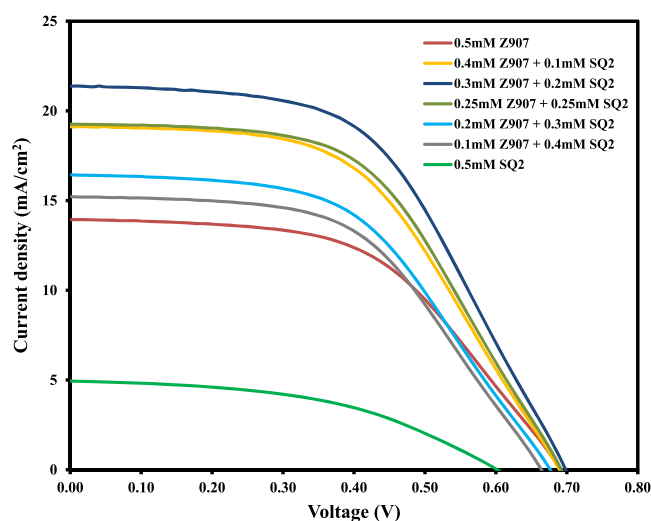

FIGURE 3 UV-Vis spectra of (A) Z907, (B) SQ2, (C) Z907 + SQ2 in ethanol, and (D) dyes adsorbed on TiO_2 films [Colour figure can be viewed at wileyonlinelibrary.com]

Z907 + SQ2 dyes adsorbed on TiO₂ is more intense, sharp, and broader in comparison with the individual dyes anchored to TiO₂ in the same conditions of fabrication. This clearly shows that the cosensitized TiO₂/(Z907 + SQ2) thin films fabricated in this experiment can absorb more photons from the incident light as compared to that of individual sensitized TiO₂/Z907 or TiO₂/SQ2 films. The more absorptions of photons leads to the more generations of electrons in the dyes adsorbed on TiO₂ semiconducting film, ie, excitation of electrons from HOMO to LUMO level of dyes, which resulted in more available conduction electrons and hence more efficiency.

3.2 | I-V characteristics of fabricated DSSC

I-V characteristics and their photovoltaic parameters of fabricated cosensitized solar cells are given in Figure 4 and Table 1, respectively. Table 1 shows the current density (J_{sc}), open circuit voltage (V_{oc}), fill factor (FF), and efficiency (η) of the fabricated solar cells. From Table 1, it can be clearly noted that the current density of the

FIGURE 4 Current-voltage characteristics of dye-sensitized solar cells [Colour figure can be viewed at wileyonlinelibrary.com]

fabricated solar cells is increased until optimized concentration, and then, it start decreasing; as for higher concentrations of SQ2, the number of available electrons is reduced because of higher bandgap of organic dye. Similarly, the open circuit voltage and FF also enhanced until optimized concentrations of dyes and then start decreasing. The overall enhanced performance has been achieved by cosensitization technique by availing both maximum absorption because of higher absorption coefficient of organic dye and more current because of less band gap of ruthenium-based dye. The results clearly show that the overall performance of cosensitized solar cells strongly depends on the concentration of cosensitizer. Under optimized conditions, the solar cell sensitized with 0.3 mM Z907 + 0.2 mM SQ2 showed J_{sc} = 21.38 mA/cm², V_{oc} = 698.37 mV, FF = 52.46%, and η = 7.83%. This PCE is significantly greater than that of the individual (TiO₂/Z907 or TiO₂/SQ2) sensitized devices. The enhancement in PCE of the cosensitized solar cell is because of the increase in J_{sc} (21.38 mA cm⁻²), V_{oc} (698.37 mV), and FF (52.46%). An increase in J_{sc} is primarily owing to strong and intense absorption of light, while the suppression of charge recombination because of cosensitization is the major cause of the increase in V_{oc}.

The uncertainty analysis of the parameters has been provided in Table 2. Five sets of each configuration have been taken to measure uncertainty or error analysis. All the parameters have been averaged over the 5 values obtained from each cell configuration. The standard deviation has been calculated to find the uncertainty or error in each parameter for each cell configuration. The overall error has been remained less than 1% among all the parameters in each cell configurations.

3.3 | EIS analysis of fabricated DSSC

Charge recombination is a major problem in solar cell devices. It is an important factor and can be understood from Figure 5A. All the dotted lines in Figure 5A

TABLE 1 Photovoltaic properties of dye-sensitized solar cells

DSSCs	J_{sc} (mA/cm²)	V_{oc} (mV)	FF (%)	η (%)
TiO₂/0.5 mM Z907	13.94	691.09	52.72	5.08
TiO₂/0.4 mM Z907 + 0.1 mM SQ2	19.12	689.65	51.62	6.81
TiO₂/0.3 mM Z907 + 0.2 mM SQ2	21.38	698.37	52.46	7.83
TiO₂/0.25 mM Z907 + 0.25 mM SQ2	19.26	692.27	52.74	7.03
TiO₂/0.2 mM Z907 + 0.3 mM SQ2	16.44	676.52	51.41	5.72
TiO₂/0.1 mM Z907 + 0.4 mM SQ2	15.22	664.04	53.05	5.36
TiO₂/0.5 mM SQ2	4.94	601.93	46.69	1.39

TABLE 2 Photovoltaic properties of dye-sensitized solar cells with error analysis

DSSCs	J_{sc} (mA/cm^2)	V_{oc} (mV)	FF (%)	η (%)
TiO$_2$/0.5 mM Z907	13.91 ± 0.31	690.95 ± 0.14	52.72 ± 0.50	5.07 ± 0.03
TiO$_2$/0.4 mM Z907 + 0.1 mM SQ2	18.97 ± 0.22	690.06 ± 0.81	51.71 ± 0.32	6.75 ± 0.06
TiO$_2$/0.3 mM Z907 + 0.2 mM SQ2	20.67 ± 0.52	698.46 ± 0.42	53.52 ± 0.91	7.72 ± 0.08
TiO$_2$/0.25 mM Z907 + 0.25 mM SQ2	19.20 ± 0.04	692.59 ± 0.22	52.64 ± 0.09	7.00 ± 0.03
TiO$_2$/0.2 mM Z907 + 0.3 mM SQ2	16.50 ± 0.12	677.04 ± 0.98	51.01 ± 0.41	5.70 ± 0.02
TiO$_2$/0.1 mM Z907 + 0.4 mM SQ2	15.23 ± 0.01	664.35 ± 0.22	52.87 ± 0.15	5.35 ± 0.01
TiO$_2$/0.5 mM SQ2	4.87 ± 0.06	600.84 ± 0.76	46.48 ± 0.41	1.36 ± 0.03
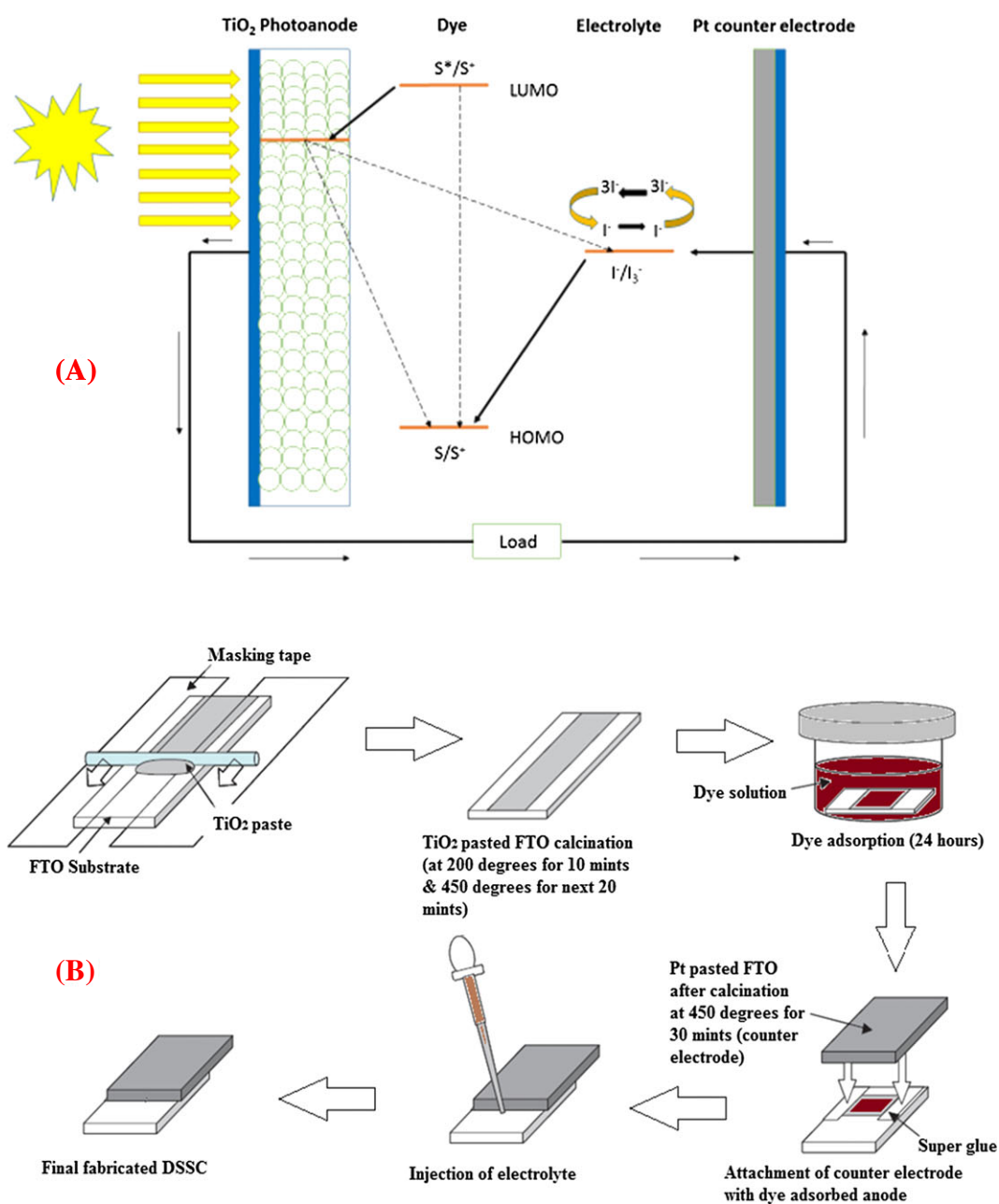
FIGURE 5 Dye-sensitized solar cells' (A) energy bandgap diagram and (B) flow diagram [Colour figure can be viewed at wileyonlinelibrary.com]

represent the various types of charge recombinations. An electron generated in response of an incident photon because of the excitation of dye, usually moved to the conduction band of the porous semiconductor. In an ideal case, an excited electron should be harvested to the external circuit; however, there are 3 possibilities. This electron can go through the following paths: either recombine with the excited dye-generated holes or transferred to semiconductor and recombine with the excited dye-generated holes or recombine with the ionized electrolyte atoms.[38] In this work, the charge recombination resistances of DSSCs were investigated by EIS analysis. Electrochemical impendence spectroscopy evaluates the response of current at different frequencies with applied AC voltage. Figure 6A, B depicts the EIS spectra (Nyquist plot) of fabricated DSSCs and the equivalent circuit of Nyquist plot, respectively. Electrochemical impendence spectroscopy spectra are represented by three semicircles. The first circle at high frequency shows interface resistance between the CE and electrolyte (R_1). The second arc at intermediate frequency and third arc at low frequency represent interface resistance between photoanode and electrolyte (R_2) and carrier transport internally inside the electrolyte through diffusion of redox couple (Z_w), respectively.[24] In Figure 6B, equivalent circuit of the Nyquist plot contains R_s, the series resistance, ie, the value of resistance representing the initial point of the first arc at high frequency in Nyquist plot. The resistances R_1 and R_2 show the resistance at back electrode/electrolyte interface and the recombination rate at anode/electrolyte interface, respectively. The symbols
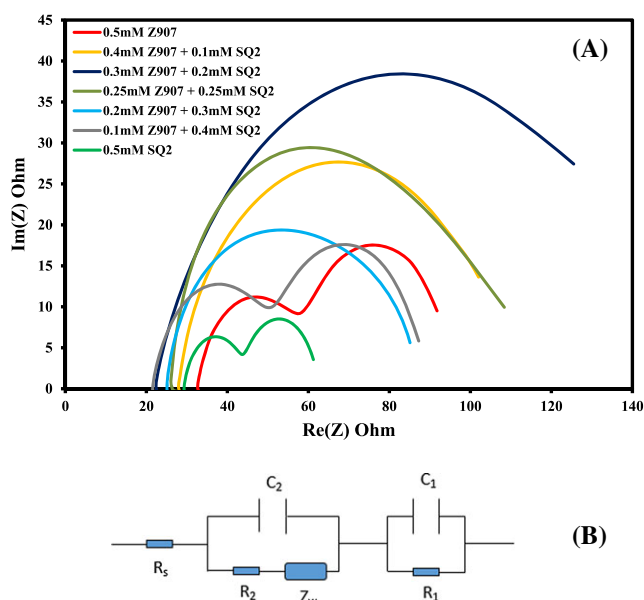
TABLE 3 Charge recombination resistance at anode interface (TiO_2/dye/electrolyte)

Sample No.	DSSCs	R_2 (ohm)
1	TiO_2/0.5 mM Z907	36
2	TiO_2/0.4 mM Z907 + 0.1 mM SQ2	81
3	TiO_2/0.3 mM Z907 + 0.2 mM SQ2	122
4	TiO_2/0.25 mM Z907 + 0.25 mM SQ2	90
5	TiO_2/0.2 mM Z907 + 0.3 mM SQ2	62
6	TiO_2/0.1 mM Z907 + 0.4 mM SQ2	41
7	TiO_2/0.5 mM SQ2	31

C_2 and C_1 indicate the capacitances (constant phase elements) to the respective interfaces, ie, anode/electrolyte and CE/electrode. The Z_w indicates the Warburg diffusion impedance. In our case, it is clear from Figure 6 that only second arc (R_2) representing resistance at photoanode/dye/electrolyte appears in 4 devices, and remaining 2 small arcs may be overshadowed by second arc.[39,40] However, the other 3 devices showed 2 arcs related to R_1 and R_2. Moreover, the R_2 denotes the recombination resistance to the free carriers at anode/electrolyte interface.[1,24] The higher the free carrier recombination resistance, the larger will be the electron lifetime and vice versa.[41] The charge recombination resistances are listed in Table 3. It can be observed from Table 3 and Figure 6 that the R_2 of 0.3 mM Z907 + 0.2 mM SQ2-sensitized DSSC possesses the higher resistance to the recombination of free charges and hence longer electron transport lifetime which is verified from the increase in the efficiency. From Table 3, it can also be noted that the individual dyes have less charge recombination resistances as compared to the cosensitized configurations of the fabricated solar cells which shows the effectiveness of cosensitization technique. The increase in electron lifetime by cosensitization can be ascribed to the enhancement of surface coverage by dye on TiO_2. The higher the surface coverage by the dye, the less will be the electron approach to TiO_2 and hence reduces the recombination process. Physically, we can explain this recombination process as shown in Figure 5A. The more coverage of TiO_2 surface with dye will lead to more generation of electrons as well as less charge recombination because of the exposure of electrolyte to the TiO_2 surface and hence enhancement of overall performance of the cosensitized configuration of fabricated solar cells.

FIGURE 6 Electrochemical impendence spectroscopy investigation of dye-sensitized solar cells and the equivalent of Nyquist plot [Colour figure can be viewed at wileyonlinelibrary.com]

4 | CONCLUSION

In this work, we used cosensitization approach to enhance the performance of DSSC. We used organic

sensitizer SQ2 as a cosensitizer with ruthenium-based dye Z907. Dye solutions of seven different concentrations were prepared for the fabrication of DSSC. The fabricated DSSC was characterized by UV-Vis spectroscopy, I-V characteristics, and EIS analysis. Our main findings are below:

- Our study demonstrated that the cosensitization approach is a highly effective method to boost the photovoltaic performance of a DSSC.
- Our results proved that the absorption of dye solution increases with the increase of SQ2 contents. However, spectra become more intense, sharp, and broader when anchored to TiO_2 film coated on the FTO surface.
- It has been also observed that the PCE, V_{oc}, J_{sc}, FF, and charge recombination resistance of solar cells strongly depend on the concentration of SQ2 dye. Under optimal conditions, the DSSC assembled with 0.3 mM Z907 + 0.2 mM SQ2 delivered PCE of 7.83%, which is significantly higher than the individual sensitized solar cell (Z907 = 5.08% and SQ2 = 1.39%).
- Our results also confirmed that the charge recombination resistance at photoanode/dye/electrolyte interface increases with cosensitization and thus reduces the dark current.

ORCID

M. Younas 🔟 http://orcid.org/0000-0002-8305-229X
M.A. Gondal 🔟 http://orcid.org/0000-0001-9570-4569

REFERENCES

1. Mehmood U, Ahmed S, Hussein IA, Harrabi K. Co-sensitization of TiO_2-MWCNTs hybrid anode for efficient dye-sensitized solar cells. *Electrochim Acta*. 2015;173:607-612.

2. Hasanuzzaman M, Rahim NA, Saidur R, Kazi SN. Energy savings and emissions reductions for rewinding and replacement of industrial motor. *Energy*. 2011;36(1):233-240.

3. Hasanuzzaman M, Rahim NA, Hosenuzzaman M, Saidur R, Mahbubul IM, Rashid MM. Energy savings in the combustion based process heating in industrial sector. *Renew Sustain Energy Rev*. 2012;16(7):4527-4536.

4. Mehmood U, Hussein IA, Harrabi K, Mekki MB, Ahmed S, Tabet N. Hybrid TiO_2–multiwall carbon nanotube (MWCNTs) photoanodes for efficient dye sensitized solar cells (DSSCs). *Sol Energy Mater Sol Cells*. 2015;140:174-179.

5. Mehmood U, Rahman S-u, Harrabi K, Hussein IA, Reddy BVS. Recent advances in dye sensitized solar cells. *Adv Mater Sci Eng*. 2014;2014:12.

6. Canadell JG, Le Quere C, Raupach MR, et al. Contributions to accelerating atmospheric CO_2 growth from economic activity, carbon intensity, and efficiency of natural sinks. *Proc Natl Acad Sci*. 2007;104(47):18866-18870.

7. Yang M-Q, Zhang N, Pagliaro M, Xu Y-J. Artificial photosynthesis over graphene–semiconductor composites. Are we getting better? *Chem Soc Rev*. 2014;43(24):8240-8254.

8. Barnham KWJ, Mazzer M, Clive B. Resolving the energy crisis: Nuclear or photovoltaics? *Nat Mater*. 2006;5(3):161-164.

9. Yan J, Saunders BR. Third-generation solar cells: A review and comparison of polymer: Fullerene, hybrid polymer and perovskite solar cells. *RSC Adv*. 2014;4(82):43286-43314.

10. O'Regan B, Grätzel M. A low-cost, high-efficiency solar cell based on dye-sensitized colloidal TiO_2 films. *Nature*. 1991;353(6346):737-740.

11. Bashir M, Ali H, Amber K, et al. Performance investigation of photovoltaic modules by back surface water cooling. *Therm Sci*. 2016;(00):290-290.

12. Yeoh M-E, Chan K-Y. Recent advances in photo-anode for dye-sensitized solar cells: A review. *Int J Energy Res*. 2017;41(15):2446-2467.

13. Wei W, Stacchiola DJ, Hu YH. 3D graphene from CO 2 and K as an excellent counter electrode for dye-sensitized solar cells. *Int J Energy Res*. 2017;41(15):2502-2508.

14. Bella F, Ozzello ED, Bianco S, Bongiovanni R. Photopolymerization of acrylic/methacrylic gel–polymer electrolyte membranes for dye-sensitized solar cells. *Chem Eng J*. 2013;225:873-879.

15. Gerosa M, Sacco A, Scalia A, et al. Toward totally flexible dye-sensitized solar cells based on titanium grids and polymeric electrolyte. *IEEE J Photovoltaics*. 2016;6(2):498-505.

16. Bella F, Verna A, Gerbaldi C. Patterning dye-sensitized solar cell photoanodes through a polymeric approach: A perspective. *Mater Sci Semicond Process*. 2018;73:92-98.

17. Bella F, Popovic J, Lamberti A, Tresso E, Gerbaldi C, Maier J. Interfacial effects in solid–liquid electrolytes for improved stability and performance of dye-sensitized solar cells. *ACS Appl Mater Interfaces*. 2017;9(43):37797-37803.

18. Ilyas AM, Gondal MA, Baig U, Akhtar S, Yamani ZH. Photovoltaic performance and photocatalytic activity of facile synthesized graphene decorated TiO_2 monohybrid using nanosecond pulsed ablation in liquid technique. *Sol Energy*. 2016;137:246-255.

19. Gondal MA, Ilyas AM, Baig U. Facile synthesis of silicon carbide-titanium dioxide semiconducting nanocomposite using pulsed laser ablation technique and its performance in photovoltaic dye sensitized solar cell and photocatalytic water purification. *Appl Surf Sci*. 2016;378:8-14.

20. Gondal MA, Ilyas AM, Fasasi TA, et al. Synthesis of green TiO 2/ZnO/CdS hybrid nano-catalyst for efficient light harvesting

using an elegant pulsed laser ablation in liquids method. *Appl Surf Sci*. 2015;357:2217-2222.

21. Kakiage K, Aoyama Y, Yano T, Oya K, Fujisawa J, Hanaya M. Highly-efficient dye-sensitized solar cells with collaborative sensitization by silyl-anchor and carboxy-anchor dyes. *Chem Commun*. 2015;51(88):15894-15897.

22. Hagfeldt A, Boschloo G, Sun L, Kloo L, Pettersson H. Dye-sensitized solar cells. *Chem Rev*. 2010;110(11):6595-6663.

23. Yum J-H, Jang S-R, Walter P, et al. Efficient co-sensitization of nanocrystalline TiO(2) films by organic sensitizers. *Chem Commun (Camb)*. 2007;(44):4680-4682.

24. Mehmood U, Hussein IA, Harrabi K, Tabet N, Berdiyorov GR. Enhanced photovoltaic performance with co-sensitization of a ruthenium(ii) sensitizer and an organic dye in dye-sensitized solar cells. *RSC Adv*. 2016;6(10):7897-7901.

25. Singh SP, Chandrasekharam M, Gupta KSV, Islam A, Han L, Sharma GD. Co-sensitization of amphiphilic ruthenium (II) sensitizer with a metal free organic dye: Improved photovoltaic performance of dye sensitized solar cells. *Org Electron*. 2013;14(5):1237-1241.

26. Lan C-M, Wu H-P, Pan T-Y, et al. Enhanced photovoltaic performance with co-sensitization of porphyrin and an organic dye in dye-sensitized solar cells. *Energ Environ Sci*. 2012;5(4):6460.

27. Wu H-P, Ou Z-W, Pan T-Y, et al. Molecular engineering of cocktail co-sensitization for efficient panchromatic porphyrin-sensitized solar cells. *Energ Environ Sci*. 2012;5(12):9843.

28. Ozawa H, Shimizu R, Arakawa H. Significant improvement in the conversion efficiency of black-dye-based dye-sensitized solar cells by cosensitization with organic dye. *RSC Adv*. 2012;2(8):3198.

29. Wei L, Yang Y, Fan R, et al. Enhance the performance of dye-sensitized solar cells by co-sensitization of 2,6-bis (iminoalkyl) pyridine and N719. *RSC Adv*. 2013;3(48):25908.

30. Sharma GD, Zervaki GE, Angaridis PA, et al. Stepwise co-sensitization as a useful tool for enhancement of power conversion efficiency of dye-sensitized solar cells: The case of an unsymmetrical porphyrin dyad and a metal-free organic dye. *Org Electron*. 2014;15(7):1324-1337.

31. Clifford JN, Forneli A, Chen H, Torres T, Tan S, Palomares E. Co-sensitized DSCs: Dye selection criteria for optimized device Voc and efficiency. *J Mater Chem*. 2011;21(6):1693-1696.

32. Kimura M, Nomoto H, Masaki N, Mori S. Dye molecules for simple co-sensitization process: Fabrication of mixed-dye-sensitized solar cells. *Angew Chem Int Ed Engl*. 2012;51(18):4371-4374.

33. Jin L, Ding ZL, Chen DJ. Zinc octacarboxylic phthalocyanine/ lutein dyads co-adsorbed nanocrystalline TiO$_2$ electrode: Enhancement in photovoltaic performance of dye-sensitized solar cells. *J Mater Sci*. 2013;48(14):4883-4891.

34. Chen Y, Zeng Z, Li C, et al. Highly efficient co-sensitization of nanocrystalline TiO$_2$ electrodes with plural organic dyes. *New J Chem*. 2005;29(6):773.

35. Kuang D, Walter P, Nüesch F, et al. Co-sensitization of organic dyes for efficient ionic liquid electrolyte-based dye-sensitized solar cells. *Langmuir*. 2007;23(22):10906-10909.

36. Wu W, Meng F, Li J, Teng X, Hua J. Co-sensitization with near-IR absorbing cyanine dye to improve photoelectric conversion of dye-sensitized solar cells. *Synth Met*. 2009;159(11):1028-1033.

37. Lee K-M, Hsu Y-C, Ikegami M, et al. Co-sensitization promoted light harvesting for plastic dye-sensitized solar cells. *J Power Sources*. 2011;196(4):2416-2421.

38. Ondersma JW, Hamann TW. Recombination and redox couples in dye-sensitized solar cells. *Coord Chem Rev*. 2013;257(9-10):1533-1543.

39. Li S, Lin Y, Tan W, et al. Preparation and performance of dye-sensitized solar cells based on ZnO-modified TiO$_2$ electrodes. *Int J Miner Metall Mater*. 2010;17(1):92-97.

40. Nair AS, Jose R, Shengyuan Y, Ramakrishna S. A simple recipe for an efficient TiO$_2$ nanofiber-based dye-sensitized solar cell. *J Colloid Interface Sci*. 2011;353(1):39-45.

41. Mehmood U, Ahmed S, Hussein IA, Harrabi K. Improving the efficiency of dye sensitized solar cells by TiO$_2$–graphene nano-composite photoanode. *Photonics Nanostructures - Fundam Appl*. 2015;16:34-42.